Broad glutamine pathway inhibition by DRP-104 results in anti-tumor activity in hypermetabolic lung tumors resistant to PD-1 or osimertinib therapy.

1572

Morgan Brady[1], Milica Momcilovic[1], Chiara Montemurro[1], Yumi Yokoyama[7], Heather Christofk[3,4,5], Katerina Politi[6], Margaret Dugan[7], Aaron Lisberg[2,5], Robert Wild[7] and David B. Shackelford[1,5*]

[1]Division of Pulmonary and Critical Care Medicine, [2]Division of Hematology and Oncology; Department of Medicine; [3]Department of Biological Chemistry; [4]UCLA Metabolomics Center; [5]Jonsson Comprehensive Cancer Center; David Geffen School of Medicine at the University of California, Los Angeles, CA 90095; [6]Department of Pathology, Yale School of Medicine, New Haven, CT 06520, USA; Yale Cancer Center, Yale School of Medicine, New Haven, CT 06520, USA; Department of Medicine, Yale School of Medicine, New Haven, CT 06520, USA; [7]Dracen Pharmaceuticals Inc., 780 Third Ave., New York, NY, 10017
*Corresponding author: David B. Shackelford Ph.D. email: DShackelford@mednet.ucla.edu

Abstract:

Recent breakthroughs with checkpoint inhibitors (CPI) or the third generation tyrosine kinase inhibitor (TKI) osimertinib (OSI) for patients with specific mutations to the epidermal growth factor receptor (EGFR) gene are now able to induce durable responses in non-small cell lung cancer (NSCLC) patients[1,2]. However, the majority of patients who receive CPI or OSI will be either non-responsive to treatment or develop therapy resistance. We sought to identify alternative treatment strategies to overcome therapy resistance by targeting metabolism in aggressive tumors. The fast rate of growth in therapy-resistant hyper-metabolic tumors (HMTs) makes them dependent on nutrients to sustain anabolic growth. To demonstrate this dependency, we coupled PET imaging using ^{18}F-FDG and ^{11}C-Glutamine (^{11}C-GLN) with in vivo metabolomics and identified a conserved metabolic signature in which lung squamous cell carcinomas (LUSC) and EGFR mutant lung adenocarcinomas (LUAD) were marked by dependence upon both glucose and glutamine[3,4]. Importantly, this metabolic signature is predictive of either response or resistance to targeted therapies that inhibit glucose and glutamine metabolism that may be exploited in a clinical setting.

We previously reported that combined targeting of glucose and glutamine metabolism with mTOR kinase inhibitor TAK228 or TKI in combination with the selective glutaminase (GLS) inhibitor CB-839 was required to significantly suppress glucose and glutamine metabolism in both LUSC and EGFR mutant LUADs resulting in metabolic crisis and tumor cell death[3,5]. Here, we tested the novel broad acting glutamine antagonist DRP-104 (sirpiglenastat) in mouse models of lung cancer as a single agent in OSI-resistant EGFR mutant LUAD or in combination with anti-PD-1 in CPI-resistant LUSC.

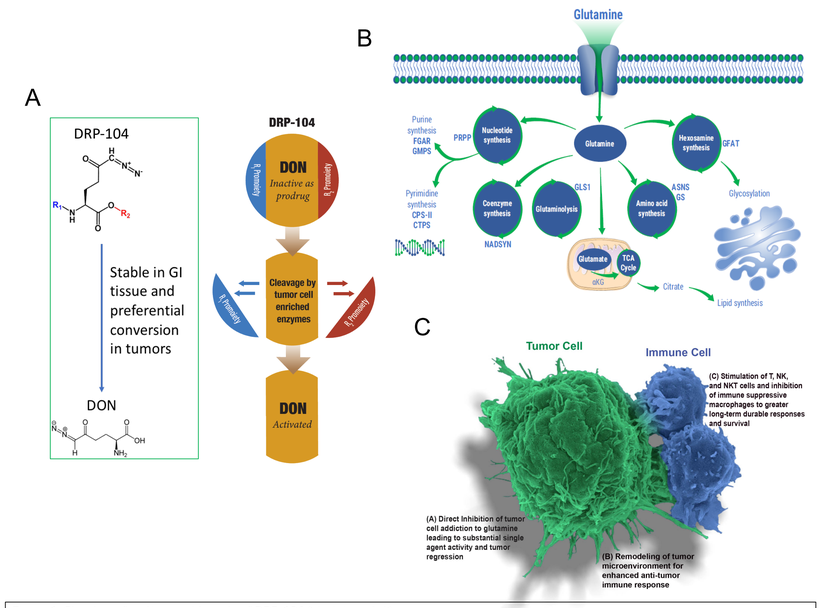

Figure 1. Structure, function, and targets of DRP-104 (sirpiglenastat).
(A) DRP-104 is a prodrug of the broad acting glutamine antagonist DON (6-Diazo-5-oxo-L-norleucine). DRP-104 is inactive in its prodrug form with high plasma and GI tissue stability. DRP-104 is preferentially distributed in tumors where it is bio-transformed and activated to the active moiety DON. *(B)* Multiple glutamine dependent pathways are inhibited by DON (Lemberg KM, *et al.,* Mol Cancer Ther 2018) *(C)* Model of MOA of DRP-104.

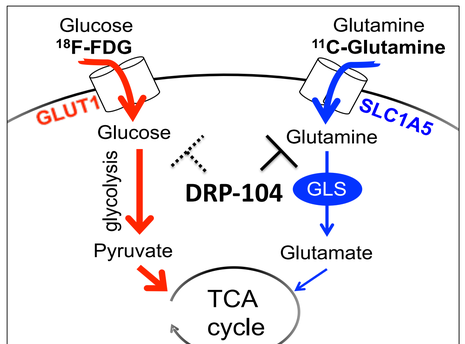

Figure 2. Glucose and glutamine dependencies in hyper-metabolic tumors (HMTs).
Proposed mechanism of DRP-104, directly inhibiting glutaminolysis and indirectly impacting glycolysis (Leone RD, *et al.,* Science 2019).

Figure 4. Evaluation of DRP-104 in patient derived xenografts of LUSC and OSI-resistant EGFR-mutant LUAD.
(A and B) LUSC PDX007 and PDX005 were treated with vehicle, 1mg/kg DRP-104, or 3mg/kg DRP-104 for 9 days (PDX007) or 13 days (PDX005). Top images are representative images of tumors stained for antibodies against GLUT1 and SLC1A5[3]. Graphs show tumor growth curve. Tumor volumes were measured three times per week with calipers. For all experiments mice received daily treatments either vehicle or DRP-104 (1 or 3mg/kg/s.c./q.d.) 5 days ON, 2 days OFF. *(C)* EGFR-mutant LUAD PDX-YLR-086 is resistant to OSI treatment and responsive to treatment with DRP-104. PDX-YLR086 was treated with vehicle, 1.4mg/kg DRP-104, 3mg/kg DRP-104, 25mg/kg OSI, or combination of 1.4mg/kg DRP-104 and 25mg/kg OSI. Graph shows tumor growth curve. Tumor volumes were measured with calipers three times per week. For all experiments mice received daily treatments either vehicle, DRP-104 (1.4 or 3mg/kg/s.c./q.d.) 5 days ON, 2 days OFF, or OSI (25mg/kg/p.o./q.d.). The data are represented as the mean +/- SEM. Statistical significance (*p<0.05; **p<0.01; ***<0.001; ****<0.0001) and analyzed via one-way ANOVA with post-hoc Dunnett's correction.

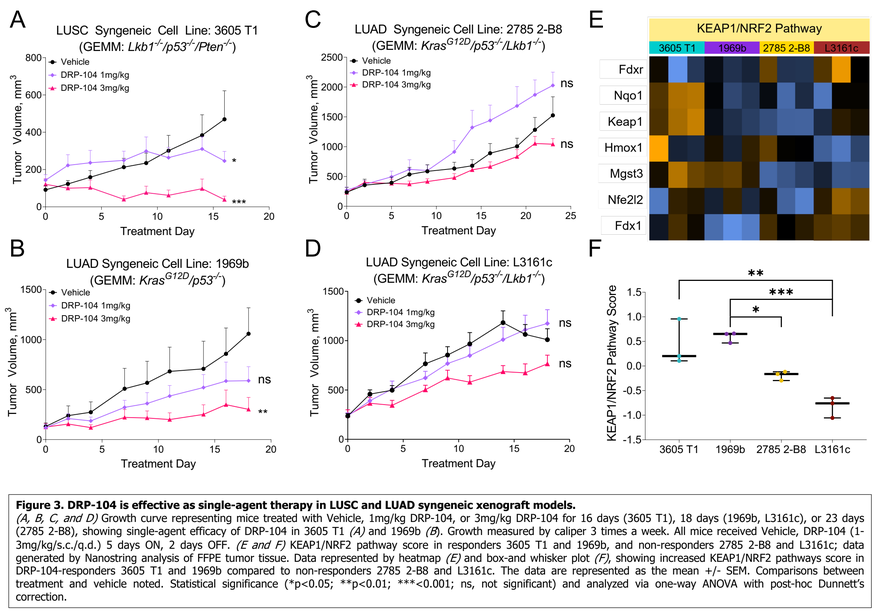

Figure 3. DRP-104 is effective as single-agent therapy in LUSC and LUAD syngeneic xenograft models.
(A, B, C, and D) Growth curve representing mice treated with Vehicle, 1mg/kg DRP-104, or 3mg/kg DRP-104 for 16 days (3605 T1), 18 days (1969b, L3161c), or 23 days (2785 2-B8), showing single-agent efficacy of DRP-104 in 3605 T1 *(A)* and 1969b *(B)*. Growth measured by caliper 3 times a week. All mice received Vehicle, DRP-104 (1-3mg/kg/s.c./q.d.) 5 days ON, 2 days OFF. *(E and F)* KEAP1/NRF2 pathway score in responders 3605 T1 and 1969b, and non-responders 2785 2-B8 and L3161c; data generated by Nanostring analysis of FFPE tumor tissue. Data represented by heatmap *(E)* and box-and whisker plot *(F)*, showing increased KEAP1/NRF2 pathways score in DRP-104-responders 3605 T1 and 1969b compared to non-responders 2785 2-B8 and L3161c. The data are represented as the mean +/- SEM. Comparisons between treatment and vehicle noted. Statistical significance (*p<0.05; **p<0.01; ***<0.001; ns, not significant) and analyzed via one-way ANOVA with post-hoc Dunnett's correction.

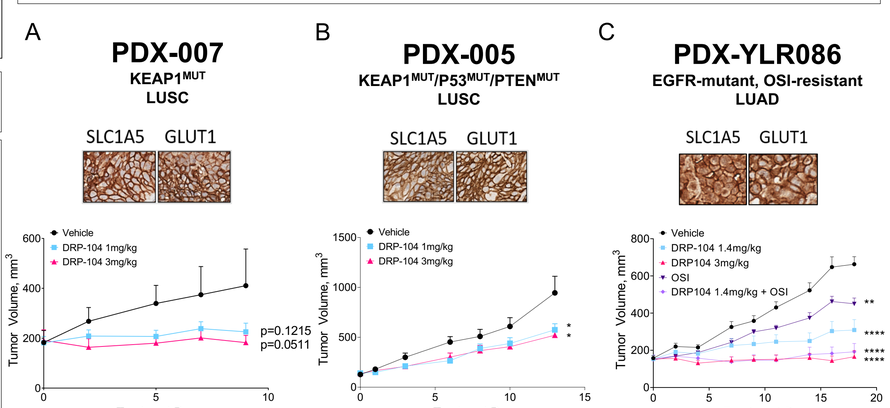

ID	Histology	Type	Identified Genetic Mutations	Response to DRP-104
Human Xenograft and PDX Tumor Models				
PDX007	LUSC	PDX	*KEAP1$^{M317V, V316A, E306Q}$*	Responder
PDX005	LUSC	PDX	*KEAP1$^{N438S, R362Q, S275A}$/p53$^{V41L, Q33K, P33R}$/PTEN^{A97S}*	Partial responder
RH2	LUSC	Xenograft	*KRAS^{Q61H}/LKB1^{Q37X}/KEAP1^{D236H}/p53^{C33R}*	Partial responder
HCC15	LUSC	Xenograft	*LKB1 (large del)/KEAP1^{G364C}/p53^{D259V}*	Partial responder
YLR086	LUAD	PDX	*EGFR^{L747_A750}* (del19)	Responder
A549	LUAD	Xenograft	*KRAS^{G12S}/LKB1^{Q37}/KEAP1^{G333C}*	Partial responder
H1437	LUAD	Xenograft	*LKB1* (p.E98-G155 del)	Partial responder
H1944	LUAD	Xenograft	*KRAS^{G12C}/LKB1^{K62N}/KEAP1^{R272L}*	Partial responder
PDX013-CR	LUAD	PDX	*KEAP1$^{G417V, M317V, V316A, E306Q}$/PTEN$^{C65S, S89P, A97S, S129G}$*	Partial responder
PDX013	LUAD	PDX	*KEAP1^{G417V}/PTEN$^{V38L, C65S, S129G}$*	Non-responder
H1568	LUAD	Xenograft	*LKB1* (del)	Non-responder
Mouse Syngeneic Tumor Models				
3605 T1	LUSC	Syngeneic cell line	*Lkb1$^{lox/lox}$/p53$^{lox/lox}$/Pten$^{lox/lox}$*	Responder
1969b	LUAD	Syngeneic cell line	*Kras^{G12D}/p53$^{lox/lox}$*	Responder
2785 2-B8	LUAD	Syngeneic cell line	*Kras^{G12D}/p53$^{lox/lox}$/Lkb1$^{lox/lox}$*	Non-responder
L3161c	LUAD	Syngeneic cell line	*Kras^{G12D}/p53$^{lox/lox}$/Lkb1$^{lox/lox}$*	Non-responder

Table 1. Summary of DRP-104 Response in LUSC and LUAD PDX, xenograft, and syngeneic models tested.
Responder defined as ≥80% tumor growth inhibition; partial responder defined as 30-80% tumor growth inhibition; non-responder defined as 0-30% tumor growth inhibition.

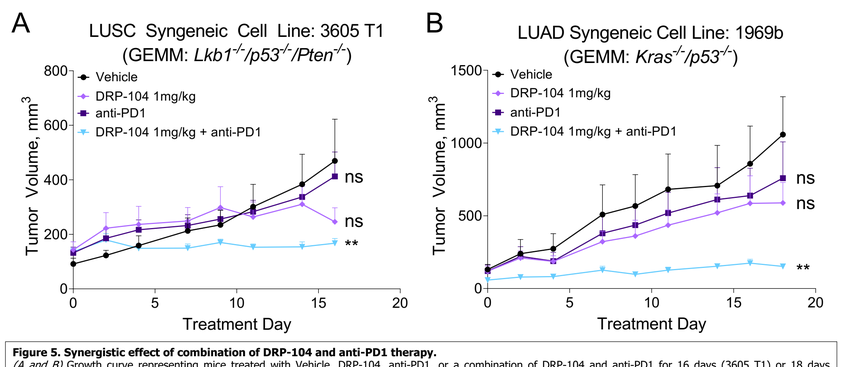

Figure 5. Synergistic effect of combination of DRP-104 and anti-PD1 therapy.
(A and B) Growth curve representing mice treated with Vehicle, DRP-104, anti-PD1, or a combination of DRP-104 and anti-PD1 for 16 days (3605 T1) or 18 days (1969b). Growth measured by caliper 3 times a week. All mice received Vehicle, DRP-104 (1mg/kg/s.c./q.d.), anti-PD1 (10mg/kg/i.p./q.4d.), or a combination of DRP-104 (1mg/kg/s.c./q.d.) and anti-PD1 (10mg/kg/i.p./q.4d.). DRP-104 was provided 5 days ON 2 days OFF. The data are represented as the mean +/- SEM. Comparisons between treatment and vehicle noted. Statistical significance (*p<0.05; **p<0.01; ns, not significant) and analyzed via one-way ANOVA with post-hoc Dunnett's correction.

Conclusions:

DRP-104 (sirpiglenastat) significantly inhibited tumor progression in the 3605 T1 (*Lkb1$^{-/-}$;Pten$^{-/-}$;p53$^{-/-}$*) and 1969b (*KRAS^{G12D};p53$^{-/-}$*) genetically engineered mouse tumor models (GEMMs) but not in the related GEMM models 2785 2-B8 (*Kras^{G12D};p53$^{-/-}$;Lkb1$^{-/-}$*) and L3161c (*Kras^{G12D};p53$^{-/-}$;Lkb1$^{-/-}$*). Responsive tumors had a higher KEAP1/NRF2 pathway score compared to non-responsive tumors. Interestingly, single agent anti-tumor activity of DRP-104 was extended into several xenograft and PDX tumor models with KEAP1 mutations, including models co-harboring mutations in KRAS, PTEN, p53 and/or LKB1. In addition, we showed that DRP-104 induced a significant response in an OSI-resistant PDX model of EGFR mutant LUAD. Lastly, in the DRP-104 responsive but anti-PD-1 non-responsive GEMM tumors, the combination of DRP-104 and anti-PD-1 treatment demonstrated therapeutic synergy, suggesting that broad inhibition of glutamine metabolism by DRP-104 induced metabolic remodeling of the tumor immune microenvironment and permissiveness to CPI blockade[6]. Overall, DRP-104 demonstrated potential to treat hypermetabolic therapy-resistant LUSC and LUAD as a single-agent therapy and in combination with immune CPI. Further clinical development of DRP-104 (sirpiglenastat) in this patient population is warranted and a first-in-human clinical trial is currently ongoing.

References:
1 Brahmer, J. *et al.* Nivolumab versus Docetaxel in Advanced Squamous-Cell Non-Small-Cell Lung Cancer. *N Engl J Med* **373**, 123-135, doi:10.1056/NEJMoa1504627 (2015).
2 Garon, E. B. *et al.* Pembrolizumab for the treatment of non-small-cell lung cancer. *N Engl J Med* **372**, 2018-2028, doi:10.1056/NEJMoa1501824 (2015).
3 Momcilovic, M. *et al.* The GSK3 Signaling Axis Regulates Adaptive Glutamine Metabolism in Lung Squamous Cell Carcinoma. *Cancer Cell* **33**, 905-921 e905, doi:10.1016/j.ccell.2018.04.002 (2018).
4 Goodwin, J. *et al.* The distinct metabolic phenotype of lung squamous cell carcinoma defines selective vulnerability to glycolytic inhibition. *Nat Commun* **8**, 15503, doi:10.1038/ncomms15503 (2017).
5 Momcilovic, M. *et al.* Targeted Inhibition of EGFR and Glutaminase Induces Metabolic Crisis in EGFR Mutant Lung Cancer. *Cell Rep* **18**, 601-610, doi:10.1016/j.celrep.2016.12.061 (2017).
6 Yokoyama, Y. *et al.* Broad acting glutamine antagonism remodels the tumor microenvironment, induces distinctive immune modulation, and synergizes with immune checkpoint blockade. Cancer Res 2020;80(16 Suppl):Abstract nr 5607.